Journal of the Physical Society of Japan **91**, 014602 (2022)
https://doi.org/10.7566/JPSJ.91.014602

Computational Investigation of the Effect of Atomic Thermal Fluctuations on the Stick-Slip Motion in Friction Force Microscopy

Yasuhiro Senda

Department of Applied Science, Yamaguchi University, Ube, Yamaguchi 755-8611, Japan

(Received April 23, 2021; accepted November 15, 2021; published online December 13, 2021)

We investigate the effect of thermal fluctuation of atoms on the stick-slip motion observed in friction force microscopy (FFM) using a computational model that couples atomic motion at the interfacial region with the torsional motion of the FFM cantilever. The proposed model enables studying friction over a wide range, starting from the atomic scale at the interface to the macroscopic scale at the cantilever. We show that the thermal fluctuation of the atoms in the interfacial region at a finite temperature aids in crossing the potential barrier, thus inducing the slip motion of the cantilever. Our results show that thermal fluctuation affects the velocity dependence of the friction force, and this result is qualitatively consistent with the thermally activated Prandtl–Tomlinson model of kinetic friction.

1. Introduction

The stick-slip (SS) phenomenon refers to a jerk-like motion often observed when two objects slide over each other.[1,2] SS motion is observed in several scenarios, ranging from macroscopic dynamics such as a rock gouge[3] and paper-on-paper systems,[4] to atomic scales such as in scanning probe microscopy.[5] In friction force microscopy (FFM), a lateral force acts on the microscope tip of cantilever when it slides over the substrate surface.[6] This sliding often induces SS motion with the periodicity of the lattice constant for layered materials such as graphite,[7,8] muscovite mica,[9] and MoS_2.[10] The sliding motion of microscope tips over ionic alkali-hallaoid surfaces also induces SS motion with lattice periodicity.[11–14] The friction force exhibits different profiles when scanning forward and backward[11] in such observations, which indicates the presence of non-conservative forces and energy dissipation. Energy dissipation has also been observed in noncontact atomic force microscopy (AFM), where dissipation maps show atomic-scale features for several surfaces.[15–23]

SS motion in sliding friction has been explained using phenomenological models[24–30] based on the Prandtl–Tomlinson (PT) model.[24,25] In the PT model, point-like tip called asperity is elastically coupled to the surface of the substance using a spring and interacts with the surface through an interaction potential such as a sinusoidal function. According to this model, if the elastic constant of the pulling spring is smaller than the curvature of the surface potential, the motion of the asperity becomes unstable. This induces SS motion in sliding friction. The instability is strongly affected by the thermal activation at the contact area. The thermally activated PT models[4,31–37] consider such thermal effects in friction processes, suitably reproducing the sliding velocity dependence of SS motion observed in FFM experiments.[11,36,38]

Although phenomenological models have been used to analyze experimental results,[10,11,39–41] the atomic behavior at contact surfaces remains unclear. In the PT model, the atoms at the probe tip are coarse-grained into a single point of elastic asperity, where the individual motion of atoms and thermal fluctuations are not considered. SS motion and frictional energy dissipation are closely associated with the atomic behavior and thermal fluctuations at contacting surfaces. Ishikawa et al. observed phonon generation and propagation at a $MoS_2(0001)$ surface.[42] However, it is difficult to realize direct and in-situ observation of atomic behavior at contact surfaces. Thus, it is challenging to investigate the effect of atomic thermal fluctuations at finite temperature on SS motion in sliding friction.

Molecular dynamics (MD) techniques are useful in investigating the thermal motion of atoms in friction processes.[43–51] Sasaki et al. studied the formation of graphene during lateral line scanning of a nanoscale tip on a multilayered graphene substrate using the molecular relaxation method.[44] The numerical approach based on Green's function MD illustrates that friction involves not only surface atoms, but also bulk atoms deep below the surface.[46,47] However, MD systems are limited by the system size and high computational time. MD techniques are often limited to the microscopic region of the local contact area, and it is difficult to study large systems, such as the macroscopic cantilever in FFM. If the motions of both atoms at the interface and the cantilever are concurrently treated, it enables us to study the friction from a wide range of view points from the atomic scale at the interface to the macroscopic scale of the cantilever. In previous studies,[49–52] we proposed a novel computational model that coupled the atomic model to the macroscopic cantilever of the AFM and FFM, where the computational models allowed us to study dissipation process in a wide range of scales. In this study, we use this computational model to investigate the effect of the thermal fluctuation of atoms on the cantilever motion and SS motion in the friction process. We use the computational model of the FFM on the ionic NaCl surface. FFM experiments for the NaCl surface show SS behavior in the atomically modulated friction and sliding velocity dependence of the friction force,[11,38] in which the thermal effects on the friction have been interpreted in terms of the above PT model.

In Sect. 2, we explain method of the computational model for the FFM. The velocity dependence of the SS motion on the NaCl surface is described and compared with the PT model in Sects. 3 and 4, we discuss the effect of the thermal fluctuation of atoms on the SS motion.

2. Computational Model of FFM

The deflection of the torsional cantilever, induced by the friction at the interface between the tip of the cantilever and

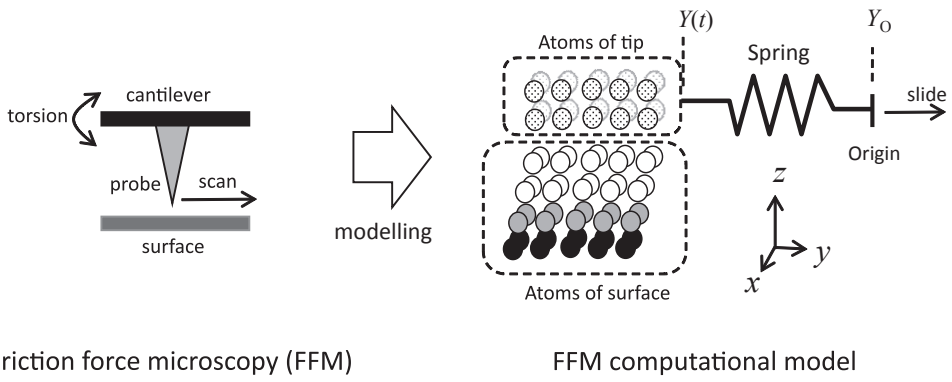

Fig. 1. Schematics of the FFM experiment and computational model. The torsional motion of the cantilever is replaced by the motion of the spring. The "frozen" atoms of the tip (meshed circles) are connected to a single spring. The atoms at the tip and surface interact with each other across the interfacial region. The atoms at the bottom of the surface (solid circles) are fixed during sliding motion. Atoms obeying the Langevin equation (gray circles) are arranged near the fixed atom. Other atoms at the surface (open circles) obey the equation of motion Eq. (2).

the surface is monitored during the FFM experiment. In the FFM computational model, the atoms at the interfacial region between the tip and the surface are described using MD, and the cantilever is replaced by a single spring, as shown in Fig. 1. The atoms at the tip are connected to the spring and shifted with the spring. The spring at the position $Y(t)$ moves along the y-axis by sliding the origin of the spring $Y_O(t)$ at constant velocity, which causes a spring displacement $\Delta Y(t) = Y(t) - Y_O(t)$. The atoms at the tip are "frozen", with no thermal fluctuation. The position of the i-th atom at the tip, $\boldsymbol{r}_i(t)$, is expressed as

$$\boldsymbol{r}_i(t) = \boldsymbol{r}_i(0) + Y(t)\boldsymbol{j}, \tag{1}$$

where $\boldsymbol{r}_i(0)$ is the initial position of the tip atoms and $\boldsymbol{j}$ is unit vector in the direction of the y-axis. The atoms at the tip contact atoms at the surface and interact with each other through the implemented interatomic potential. The motion of the i-th atom at the surface is governed by the following equation of motion

$$m_i\ddot{\boldsymbol{r}}_i = -\frac{\partial U(\{\boldsymbol{r}_i\})}{\partial \boldsymbol{r}_i}, \tag{2}$$

where $U(\{\boldsymbol{r}_i\})$ is the interatomic potential of the atomic system, as described below. The atoms at the surface are thermally fluctuated at a finite temperature. The equation for the position of the spring is given by

$$W\ddot{Y}(t) = -k\{Y(t) - Y_O(t)\} - \gamma\dot{Y}(t) + F_L(\{\boldsymbol{r}_i\}), \tag{3}$$

where W denotes the mass of the spring. The first term on the right-hand side represents the elastic force on the spring with spring constant k, the second term is the damping force with damping coefficient γ, and the third term $F_L(\{\boldsymbol{r}_i\})$ corresponds to the lateral force acting on the spring, obtained from the shear stress τ_{zy} of the atomic system. The simultaneous equations (1)–(3) for the atoms and positions of the spring are solved numerically, and the atomic trajectories and time evolution of the spring position are thus obtained.

The coordination of the atoms at the bottom layers of the surface is fixed during sliding, as shown in Fig. 1. The atoms obeying the Langevin equation are arranged near the fixed atoms. The Langevin equation incorporates friction and random forces in addition to the interatomic force. These "Langevin" atoms control the temperature in the atomic system as a heat bath. They also inhibit the reflection of phonons from the fixed atoms at the bottom layers. The normal force acting on the atomic system along the z-axis are set by modulating the height of the tip atoms in the direction of the z-axis. Periodic boundary conditions are applied to the x and y directions in the atomic system.

When the spring slides and the tip atoms are shifted, shear stress and friction force arise around the interfacial region between the tip and the surface. This situation corresponds to the sliding friction caused by the scanning of the probe in the FFM experiment.

We apply this model to FFM experiments on an ionic NaCl(001) surface,[11,38] as reported previously.[52] The FFM experiments employ silicon tips that may be contaminated by substances adhering to the surface, and the surface atoms may be transferred to the tip.[5] It has been indicated that such surface atoms on the tip are "re-organized" during scanning, which promotes the appearance of atomic SS motion.[5,53] Therefore, we assume that the tip contains NaCl ions instead of silicon atoms. The Coulombic interaction is used as the inter-atomic potential between the Na and Cl ions.[43,48,54–56] The NaCl structure with a lattice constant of 5.76 Å is set as the initial position of the ions of the tip and the surface. The tip and surface include 2048 and 3072 ions, respectively. The same normal forces are applied for all cases. MD calculations are performed using the LAMMPS software[57] with a time step $\Delta t = 2$ fs. The spring constant k is set to 890 N/m, and the mass W is 250 times the mass of the Na atom. The origin Y_O slides at the constant velocities of 0.04, 0.06, 0.08, 0.12, and 0.16 Å/ps at temperatures $T = 150$, 225, 300, 450, and 600 K. These velocities are many orders of magnitude faster than scanning speed with the order of nm/s in FFM experiments,[11] however, the velocity dependence obtained for the range of these velocities are qualitatively consistent with the thermally activated PT model, as shown in next section.

3. Results

Figure 2 illustrates the kinetic friction force F as a function of the position of the origin of the spring, together with the snapshots of the atomic model. Here, $F = k(Y - Y_O)$. The sliding of the origin of the spring causes the atoms at the tip to shift with the position of the spring. Here, shear stress is

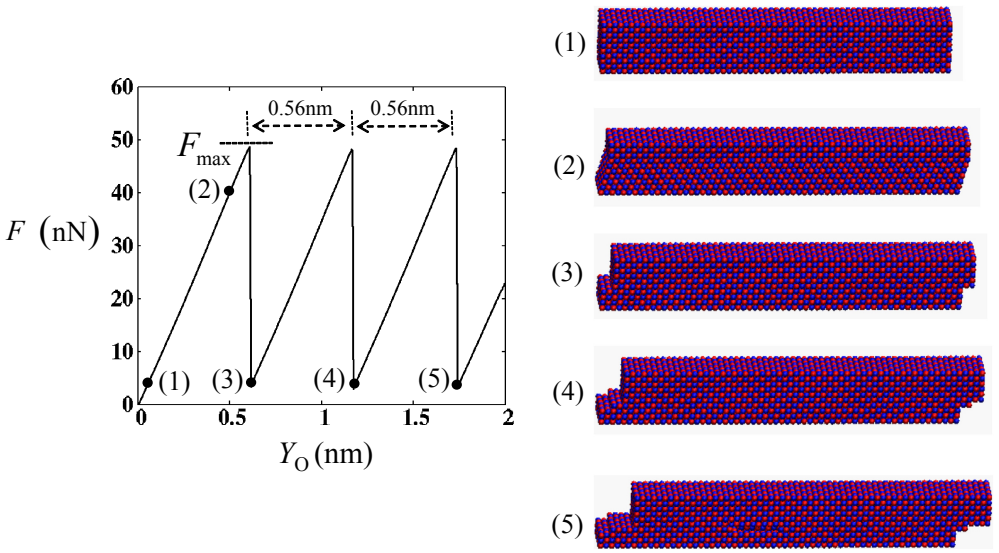

Fig. 2. (Color online) Kinetic friction force F of the present FFM model as a function of the position of the spring's origin Y_O. Snapshots of the atomic system of the FFM model at points (1)–(5) are shown.

applied to the atomic system, and it deforms the lattice structure, as shown in Fig. 2(2). The shear stress and elastic deformation in the atomic system increases with the sliding of the origin of the spring, which corresponds to the stick motion in the friction process. When the elastic deformation of the atomic system reaches the elastic limit, atoms at the interfacial region slip, accompanied by the quick motion of the spring, as shown in Fig. 2(3). The composite system of the atomic model and spring is relaxed by the slip motion, and with continuous sliding of the spring, the shear stress in the atomic model and the displacement of the spring increase again. The SS motion occurs repeatedly during the sliding of the spring, which yields a sawtooth-like profile of the friction force. At each slip motion, the ions on the slip plane slide by a distance equivalent to one lattice constant of NaCl. The form of the SS motion shown in Fig. 2 appears with a periodicity of approximately 0.56 nm, which is consistent with the lattice constant of NaCl. The strain energy of the lattice structure is released at the moment of slip, which gives rise to phonons and an increase in kinetic energy at the interface between the tip and the surface. The thermal energy generated at the interface is dissipated through the phonons in the substrate. This dissipation process has been discussed in Ref. 52. The SS motion occurs if the applied normal force is positive. Otherwise, a continuous motion of the spring appears, which is in agreement with previously reported results.[52)]

The kinetic friction force depends on the sliding velocity of the spring and the temperature in the atomic system. Figure 3 shows the force F_{max} in the SS motion as a function of the velocity at various temperatures, where the force F_{max} is defined as the maximum of the kinetic friction force at the stick motion. F_{max} increases with the sliding velocity and decreases at low temperatures.

According to the thermally activated PT model,[32–37)] the kinetic friction force $F_{PT}(v, T)$ is described as a function of the sliding velocity v and temperature T as

$$F_{PT}(v, T) = F_0 - b\left[T \ln\left(B\frac{T}{v}\right)\right]^{2/3}, \tag{4}$$

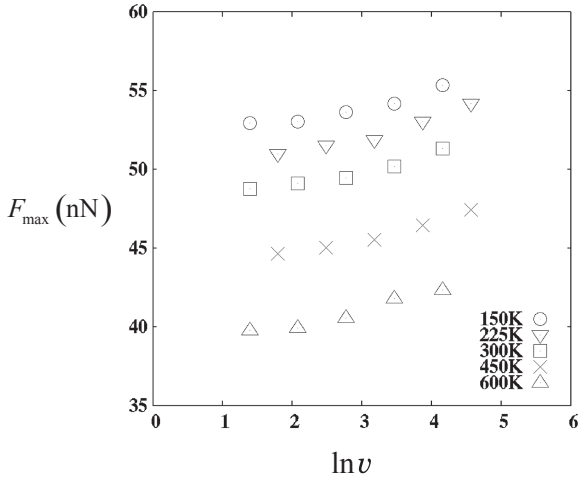

Fig. 3. F_{max} as a function of the logarithmic velocity v at various temperatures. F_{max} is defined as the maximum force of the kinetic friction force, as shown in Fig. 2.

where F_0 is the friction force at zero temperature for the low-velocity limit case, and b and B ($BT > v$) are positive parameters obtained from the spring constant, amplitude of the tip-surface potential, and damping coefficient in the thermally activated PT model, but they do not depend on T and v. For the case of constant T/v, $F_{PT}(v, T)$ is written as

$$F_{PT}(v, T) = F_0 + \text{const} * T^{2/3}. \tag{5}$$

According to the thermally activated PT model, $F_{PT}(v, T)$ exhibits a linear relationship with $T^{2/3}$ for the case of constant T/v. We obtain the friction force F_{max} from the present FFM model for the case of constant T/v, $T = 150$ K at $v = 0.04$ Å/ps, 225 K at 0.06 Å/ps, 300 K at 0.08 Å/ps, 450 K at 0.12 Å/ps, and 600 K at 0.16 Å/ps. Figure 4 shows a remarkable linearity of F_{max} with $T^{2/3}$, and extrapolating this plot to a low-velocity limit gives the value of F_0 as 60.7 nN. Equation (4) for the thermal activated PT model can be rewritten as

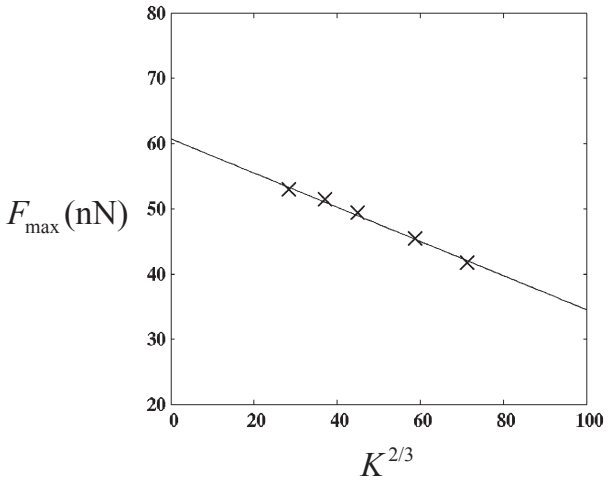

Fig. 4. F_{max} as a function of $T^{2/3}$ for the case of constant T/v, $T = 150$ K at $v = 0.04$ Å/ps, 225 K at 0.06 Å/ps, 300 K at 0.08 Å/ps, 450 K at 0.12 Å/ps, and 600 K at 0.16 Å/ps together with a straight line fit to these points.

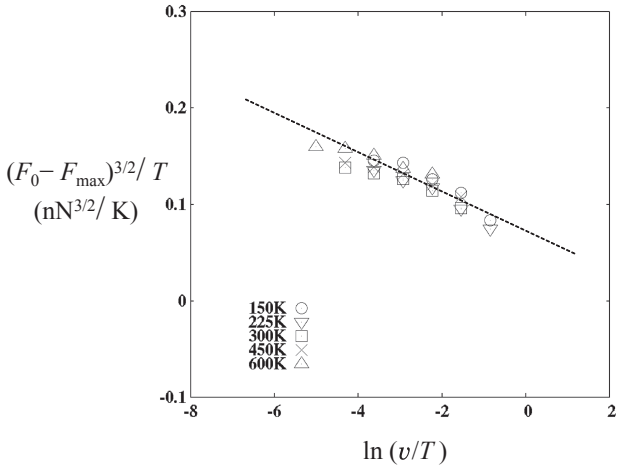

Fig. 5. Calculated $(F_0 - F_{max})^{3/2}/T$ as a function of $\ln(v/T)$. The value of F_0 is extracted from the plot in Fig. 4. The dashed line is a visual guide.

$$\frac{(F_0 - F_{PT})^{3/2}}{T} = b^{3/2}\left(\ln B - \ln \frac{v}{T}\right). \tag{6}$$

Since b and B are independent of v and T in the PT model, the above equation indicates that $(F_0 - F_{PT})^{3/2}/T$ can be described as a unique linear function of $\ln(v/T)$ at various velocities and temperatures. Using the above values of F_0 and F_{max} obtained from the present model at different temperatures with the sliding velocities, $(F_0 - F_{max})^{3/2}/T$ is plotted as a function of $\ln(v/T)$ in Fig. 5. A straight line plot with small deviations is obtained. This indicates that the velocity dependence of the friction force obtained from the present FFM model is qualitatively consistent with that of the thermal activated PT model.[32–37] The deviations arise from the difference between the two models. In the present FFM model, the atomic model is used to describe an interaction between the tip and the surface, while in the PT model, the interaction is replaced by a sinusoidal function as discussed below.

4. Discussion

Before we discuss the effect of atomic thermal fluctuations on SS motion we review the thermally activated PT model.[4,32–37] In the original PT model,[24,25] it is assumed that the asperity at the contacting surface is elastic, as shown in Fig. 6(a). The asperity interacts with the surface through an interaction potential, such as a sinusoidal function. The position of the asperity during friction is described by the state on the potential U_{PT}, comprised of the elastic potential of the asperity and the interaction potential, as shown in Fig. 6(b). If the curvature of the interaction potential is larger than the elastic constant of the asperity, the state of asperity remains at a local minimum with the potential wall (ΔU). U_{PT} is modulated as the origin of the asperity slides, and the state of the asperity remains at the local minimum until ΔU at the local minimum disappears. This corresponds to the stick state in SS motion. As the origin of the asperity slides continuously, when ΔU vanishes, the state of the asperity skips to the next minimum on U_{PT}. This corresponds to the "slip" state in the SS motion.

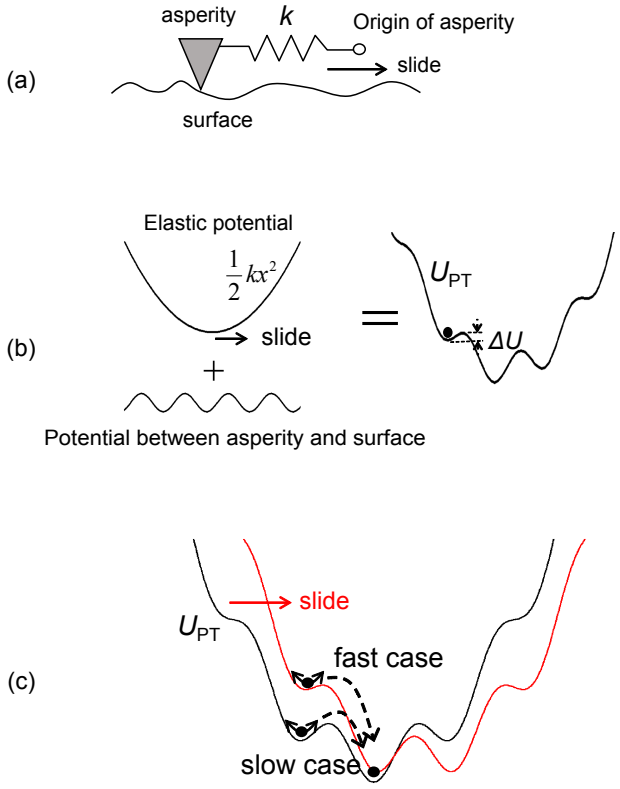

Fig. 6. (Color online) (a) Schematic of the PT model. (b) Potential of the elastic energy of the asperity $\frac{1}{2}kx^2$ and the interaction between the asperity and the surface (sinusoidal function), and the sum of two potentials U_{PT}. The position of the asperity during sliding is described by the state on the U_{PT}, as shown by the solid circle. The state is located at the local minimum with potential wall ΔU, when the asperity sticks on the surface during SS motion. (c) In the thermally activated PT model, the state of the asperity fluctuates on U_{PT} at a finite temperature. Owing to this thermal fluctuation, the state on the local minimum jumps to the next minimum. This jump in the state occurs at a higher U_{PT} for the case of fast sliding velocity.

In the thermally activated PT model, the thermal effect at a finite temperature is described by the fluctuation of the state on U_{PT}, as shown in Fig. 6(c). If the asperity slowly slides on the surface, the thermal fluctuation is enhanced, which makes the state of the asperity easily overcome ΔU to enter the next minimum on U_{PT}. By contrast, if the asperity slides faster, the fluctuation effect does not contribute significantly to over-

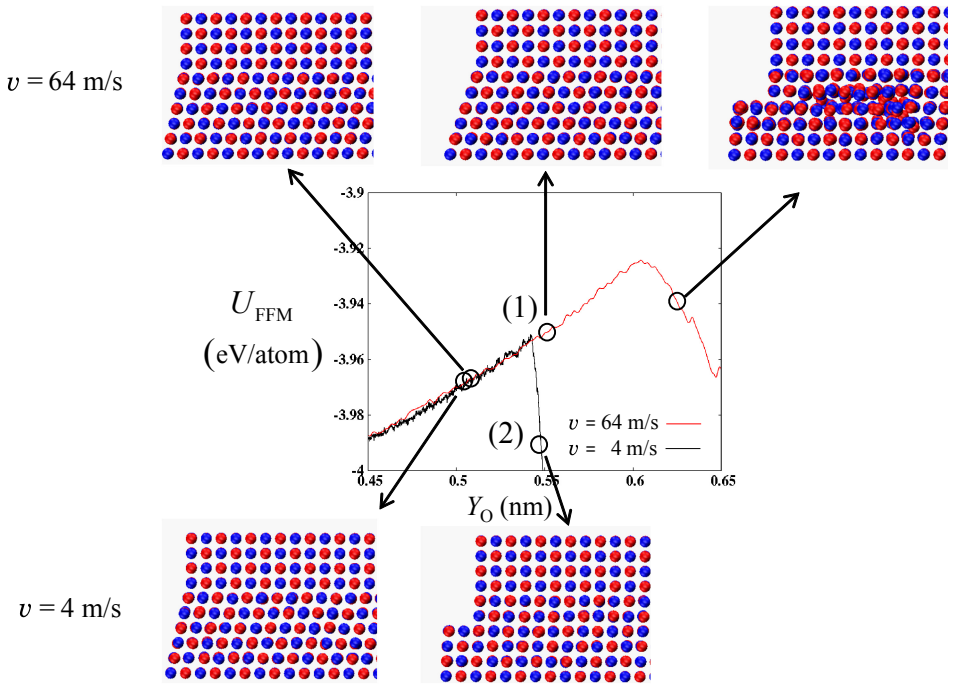

Fig. 7. (Color online) The potential energies of the atomic system and the spring as a function of the position of the spring's origin, Y_O. Snapshots of the atomic system of the FFM model at points indicated by the open circles are drawn.

coming ΔU. In this case, the state of the asperity preferably remains at the local minimum. This gives rise to the higher amount of the distortion of the asperity and the higher U_{PT}, as shown in Fig. 6(c). The above theory predicts the relationship between the kinetic friction force F and sliding velocity v, as shown in Eq. (4).

Among these PT models, the atoms of the asperity at the interfacial region are coarse-grained into a single mass point, in which motions of individual atoms of the asperity are ignored. Although the velocity dependence of the friction force obtained from the thermally activated PT model is consistent with previously reported experimental results,[11,36,38] the contribution of the motions of atoms at a finite temperature to the kinetic friction force is still unclear.

The present FFM model enables investigating the atomic motions, thermal fluctuations of the atoms and also these effects on the SS motion as follows. The potential energy of the atomic system can be calculated using the FFM model. We define the potential energy U_{FFM} of the FFM model, which is comprised of the interatomic potential $U(\{\boldsymbol{r}_i\})$ and the elastic potential energy $1/2 * k(Y - Y_O)^2$, as given by

$$U_{FFM} = U(\{\boldsymbol{r}_i\}) + \frac{1}{2}k(Y - Y_O)^2. \tag{7}$$

This U_{FFM} of the FFM model corresponds to the above U_{PT} for the thermally activated PT model. Figure 7 shows U_{FFM} as a function of Y_O. During the stick motion of the FFM model, U_{FFM} increases as the spring slides. When U_{FFM} reaches a threshold value, a slip in the NaCl crystal occurs at the interfacial region, and U_{FFM} rapidly drops at the onset of the slip motion. U_{FFM} fluctuates owing to the motion of individual atoms at a finite temperature. Rapidly fluctuating U_{FFM} appears at a low slide velocity, which induces a slip plane in the atomic system at a lower value of U_{FFM}. In contrast, for the case of a faster velocity ($v = 0.64$ m/s), the period of the fluctuation becomes longer, and the effect of the fluctuation becomes weaker. The stick state of the atomic system remains at a higher value of U_{FFM}, as illustrated in Fig. 7(1), while at the same position, the spring atoms slip in the case of lower velocity [Fig. 7(2)]. For the case of a high velocity, a higher displacement of the spring is required for the slip plane in the atomic system to become apparent. This results in the increase of the friction force in the SS mode.

The mechanism underlying the thermal fluctuation and its effects on the SS motion are common between the present FFM model and the thermally activated PT model. The threshold value of U_{FFM} of the stick state is affected by the thermal fluctuation of atoms in the FFM model. In the thermally activated PT model, the stick state of the asperity on U_{PT} overcomes the potential wall and enters the state of slip motion with the help of thermal fluctuation. The common trend between the two models reflects the fact that the results calculated from the FFM model are qualitatively consistent with those of the thermally activated PT model, as shown in Fig. 5(c). However, the system of the FFM model is quite different from that of the PT model. The state of the FFM model is fluctuated on the potential surface U_{FFM}, which has many degrees of freedom including those of the atoms, while a single mass point of the PT model fluctuates on the potential surface U_{PT}. This could give the quantitative difference, as indicated by the deviations from the straight line in Fig. 5.

In a previous work, we investigated the energy dissipation in SS motion.[52] In present work, we focus on the effects of thermal fluctuation by investigating the velocity dependence of the SS motion. The effect on the SS motion is clearly understood using the computational model, which ameliorates a limitation of conventional MD by coupling the atomic model with the motion of FFM cantilever.

The cantilever of the present model has one degree of freedom Y along the scan direction. The theoretical studies indicate that the friction system with more degrees of freedom avoids the elastic instability that causes the SS behavior. Hirano et al. proposed that the two-dimensional system avoids the region of elastic instability on the adiabatic potential, and that the discontinuous change of the atomic positions, such as SS motion, is unlikely to occur in a realistic system.[58] Washizu et al. indicated that the friction force in multilayered graphene sheets does not show SS behavior owing to the internal degree of freedom in the multilayered structure.[59] In contrast to these indications, the two-dimensional FFM on the ionic NaF(100) surface observed square-wave behavior of the cantilever motion with sharp step-like rises and falls across the scan direction, in addition to sawtooth behavior along the scan direction.[10,12] We are planning to investigate how the degrees of freedom effects the SS motion with two-dimensional motion of the cantilever.

The tip and the surface in the atomic system have the same lattice constant, which means that the surface of the tip is commensurate with that of the surface at the interface. Such a commensurate contact often leads to an increase of the friction and energy dissipation, as shown in this study. However, for the case of an incommensurate contact, lower friction is expected.[58] In incommensurate contact, the strong interaction between two surfaces induces a transition, called Aubry transition, with regions of commensurability separated by regularly spaced dislocation, where a finite energy per dislocation is required to move over the corrugated substrate.[60] The motion of dislocation produced by the Aubry transition is affected by the thermal fluctuation of atoms at the interface, as shown in the present system of the commensurate contact. There still remains scope for further investigation of the case of incommensurate contact. In addition, the interface between the tip and surface of the present system is assumed to be homogeneous and flat, containing atoms that interact mainly through the Coulombic force. However, there are different types of asperities on inhomogeneous surfaces at the atomic scale. It remains unclear whether such a realistic system shows the velocity dependence of the friction force, as seen in the present system. It is worth investigating whether the same results can be obtained on a surface containing atoms interacting via the van der Waals or metallic interactions. The thermal effect of atoms on the friction force and its velocity dependence will be investigated in a future study.

5. Conclusions

The effect of thermal fluctuation of atoms on friction and the corresponding velocity dependence have been investigated. The results obtained from the FFM model are qualitatively consistent with those of the thermally activated PT model. The present FFM model enables us to understand the effect of thermal fluctuations on friction from an atomic point of view. We find that the thermal fluctuation of atoms at a finite temperature affects the velocity dependence of the friction force during SS motion.

Acknowledgment This research has been performed under the Inter Inter-University Cooperative Research Program of the Center for Computational Materials Science, Institute for Materials Research, Tohoku University (Proposal Nos. 20K0024 and 202012-RDKGE-0003). This work used computational resources provided by Research Institute for Information Technology, Kyushu University through the HPCI System Research Project (Project ID: hp200006 and hp210018).

1) B. N. J. Persson, *Sliding Friction: Physical Principles and Applications* (Springer, Heidelberg, 1998).
2) E. Rabinowicz, *Friction and Wear of Materials* (Wiley, New York, 2013) 2nd ed.
3) Y. Gu and T. F. Wong, *Nonlinear Dynamics and Predictability of Geophysical Phenomena* (AGU, Washington, D.C., 1994) Geophysical Monograph No. 83, Vol. 18, p. 15.
4) F. Heslot, T. Baumberger, B. Perrin, B. Caroli, and C. Caroli, Phys. Rev. E **49**, 4973 (1994).
5) R. Bennewitz, Mater. Today **8** [5], 42 (2005).
6) E. Meyer, R. Overney, D. Brodbeck, L. Howald, R. Luthi, J. Frommer, and H.-J. Guntherodt, Phys. Rev. Lett. **69**, 1777 (1992).
7) C. M. Mate, G. M. McClelland, R. Erlandsson, and S. Chiang, Phys. Rev. Lett. **59**, 1942 (1987).
8) S. Kawai, A. Benassi, E. Gnecco, H. Söde, R. Pawlak, X. Feng, K. Müllen, D. Passerone, C. A. Pignedoli, P. Ruffieux, R. Fasel, and E. Meyer, Science **351**, 957 (2016).
9) R. Erlandsson, G. Hadziioannou, C. M. Mate, G. M. McClelland, and S. Chiang, J. Chem. Phys. **89**, 5190 (1988).
10) S. Fujisawa, E. Kishi, Y. Sugawara, and S. Morita, Phys. Rev. B **52**, 5302 (1995).
11) A. Socoliuc, R. Bennewitz, E. Gnecco, and E. Meyer, Phys. Rev. Lett. **92**, 134301 (2004).
12) S. Fujisawa, Y. Sugawara, and S. Morita, Philos. Mag. **74**, 1329 (1996).
13) L. Howald, H. Haefke, R. Lüthi, E. Meyer, G. Gerth, H. Rudin, and H.-J. Güntherodt, Phys. Rev. B **49**, 5651 (1994).
14) R. Lüthi, E. Meyer, M. Bammerlin, L. Howald, H. Haefke, T. Lehmann, C. Loppacher, H.-J. Güntherodt, T. Gyalog, and H. Thomas, J. Vac. Sci. Technol. B **14**, 1280 (1996).
15) R. Hoffmann, in *Noncontact Atomic Microscopy*, ed. S. Morita, F. J. Giessibl, and R. Wiesendanger (Springer, Berlin, 2009) Vol. 2, p. 86.
16) B. Anczykowski, B. Gotsmann, H. Fuchs, J. P. Cleveland, and V. B. Elings, Appl. Surf. Sci. **140**, 376 (1999).
17) R. Bennewitz, A. S. Foster, L. N. Kantorovich, M. Bammerlin, C. Loppacher, S. Schär, M. Guggisberg, E. Meyer, and A. L. Shluger, Phys. Rev. B **62**, 2074 (2000).
18) C. Loppacher, R. Bennewitz, O. Pfeiffer, M. Guggisberg, M. Bammerlin, S. Schär, V. Barwich, A. Baratoff, and E. Meyer, Phys. Rev. B **62**, 13674 (2000).
19) T. Fukuma, K. Umeda, K. Kobayashi, H. Yamada, and K. Matsushige, Jpn. J. Appl. Phys. **41**, 4903 (2002).
20) H. J. Hug and A. Baratoff, in *Noncontact Atomic Microscopy*, ed. S. Morita, R. Wiesendanger, and E. Meyer (Springer, Berlin, 2002) Chap. 20.
21) M. Ashino, R. Wiesendanger, A. N. Khlobystov, S. Berber, and D. Tomanek, Phys. Rev. Lett. **102**, 195503 (2009).
22) Y. Naitoh, Y. J. Li, H. Nomura, M. Kageshima, and Y. Sugawara, J. Phys. Soc. Jpn. **79**, 013601 (2010).
23) K. Iwata, S. Yamazaki, Y. Tani, and Y. Sugimoto, Appl. Phys. Express **6**, 055201 (2013).
24) L. Prandtl, Z. Angew. Math. Mech. **8**, 85 (1928).
25) G. A. Tomlinson, Philos. Mag. **7**, 905 (1929).
26) T. Gyalog, M. Bammerlin, R. Lüthi, E. Meyer, and H. Thomas, Europhys. Lett. **31**, 269 (1995).
27) T. Gyalog and H. Thomas, Z. Phys. B **104**, 669 (1997).
28) A. Volmer and Th. Nattermann, Z. Phys. B **104**, 363 (1997).
29) J. R. Rice and A. L. Ruina, J. Appl. Mech. **50**, 343 (1983).
30) D. Tománek, W. Zhong, and H. Thomas, Europhys. Lett. **15**, 887 (1991).
31) A. Ruina, J. Geophys. Res. **88**, 10359 (1983).
32) Y. Sang, M. Dube, and M. Grant, Phys. Rev. Lett. **87**, 174301 (2001).
33) B. N. J. Persson, O. Albohr, F. Mancosu, V. Peveri, V. N. Samoilov, and I. M. Sivebaek, Wear **254**, 835 (2003).
34) E. Riedo, E. Gnecco, R. Bennewitz, E. Meyer, and H. Brune, Phys. Rev. Lett. **91**, 084502 (2003).
35) H. Hölscher, A. Schirmeisen, and U. D. Schwarz, Philos. Trans. R. Soc.

A **366**, 1383 (2008).
36) L. Jansen, H. Hölscher, H. Fuchs, and A. Schirmeisen, Phys. Rev. Lett. **104**, 256101 (2010).
37) A. Vanossi, N. Manini, M. Urbakh, S. Zapperi, and E. Tosatti, Rev. Mod. Phys. **85**, 529 (2013).
38) E. Gnecco, R. Bennewitz, T. Gyalog, Ch. Loppacher, M. Bammerlin, E. Meyer, and H.-J. Güntherodt, Phys. Rev. Lett. **84**, 1172 (2000).
39) D. Inoue, S. Machida, J. Taniguchi, and M. Suzuki, Phys. Rev. B **86**, 115411 (2012).
40) S. Kawai, N. Sasaki, and H. Kawakatsu, Phys. Rev. B **79**, 195412 (2009).
41) H. Hölscher, U. D. Schwarz, and R. Wiesendanger, Surf. Sci. **375**, 395 (1997).
42) M. Ishikawa, N. Wada, T. Miyakawa, H. Matsukawa, M. Suzuki, N. Sasaki, and K. Miura, Phys. Rev. B **93**, 201401 (2016).
43) A. L. Shluger, A. L. Rohl, D. H. Gay, and R. T. Williams, J. Phys.: Condens. Matter **6**, 1825 (1994).
44) N. Sasaki, H. Okamoto, N. Itamura, and K. Miura, e-J. Surf. Sci. Nanotechnol. **7**, 173 (2009).
45) N. Sasaki, T. Ando, S. Masuda, H. Okamoto, N. Itamura, and K. Miura, e-J. Surf. Sci. Nanotechnol. **14**, 204 (2016).
46) S. Kajita, H. Washizu, and T. Ohmori, Europhys. Lett. **87**, 66002 (2009).
47) S. Kajita, Phys. Rev. E **94**, 033301 (2016).
48) F. F. Canova and A. S. Foster, Nanotechnology **22**, 045702 (2011).
49) Y. Senda, N. Imahashi, S. Shimamura, J. Blomqvist, and R. M. Nieminen, e-J. Surf. Sci. Nanotechnol. **12**, 339 (2014).
50) Y. Senda, J. Blomqvist, and R. Nieminen, J. Phys.: Condens. Matter **28**, 375001 (2016).
51) Y. Senda, J. Blomqvist, and R. M. Nieminen, e-J. Surf. Sci. Nanotechnol. **16**, 132 (2018).
52) Y. Senda, Appl. Phys. Express **12**, 045505 (2019).
53) A. I. Livshits and A. L. Shluger, Phys. Rev. B **56**, 12482 (1997).
54) S. Kawai, F. F. Canova, T. Glatzel, A. S. Foster, and E. Meyer, Phys. Rev. B **84**, 115415 (2011).
55) M. J. L. Sangster and R. M. Atwood, J. Phys. C **11**, 1541 (1978).
56) R. W. Grimes, C. R. A. Catlow, and A. M. Stoneham, J. Phys.: Condens. Matter **1**, 7367 (1989).
57) S. Plimpton, J. Comput. Phys. **117**, 1 (1995).
58) M. Hirano and K. Shinjo, Phys. Rev. B **41**, 11837 (1990).
59) H. Washizu, S. Kajita, M. Tohyama, T. Ohmori, N. Nishino, H. Teranishi, and A. Suzuki, Faraday Discuss. **156**, 279 (2012).
60) M. Peyrard and S. Aubry, J. Phys. C **16**, 1593 (1983).